



ESS2222H

**Tectonics and Planetary Dynamics
Lecture 5 – The Structure of the Earth**

Hosein Shahnas

University of Toronto, Department of Earth Sciences,

The Structure of the Earth

The determination of elastic parameters and density throughout the Earth using observations of seismic waves and other constraints is the prototype **inverse problem** in geophysics.

Inverse Problem:

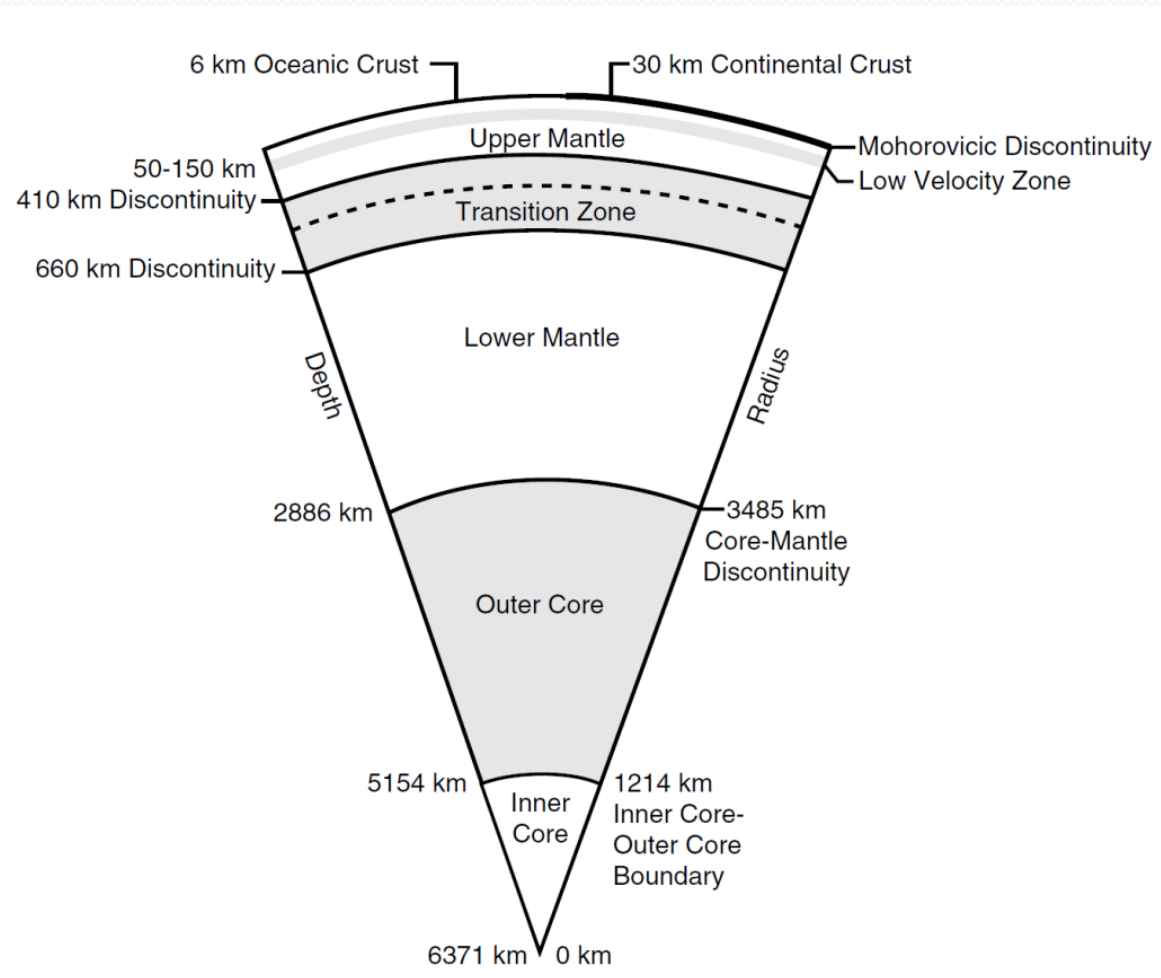
An inverse problem in engineering and science is a problem solving based on observations (effects). We start from the effects and try to estimate the cause. Density profile calculation in the interior of Earth is an example.



The Structure of the Earth

Difficulties:

- a) Non-uniqueness
- b) Incomplete sampling
- c) Errors in data



The Structure of the Earth

Oceanic crust:

Basaltic composition – volcanic-**mafic** rock (**low silica** (SiO_2)) → low viscous- so it can more spread), rich in **magnesium** and **ferric iron**). $\bar{d} \sim 6 \text{ km}$

Because of heavy **metal content**, its **density** is **higher** than the continental crust and can be subducted easier than the continental crust.

Continental crust:

Silicic composition – because of higher amount of silicon oxide (SiO_2) the **density** of the continental crust is **lower** than the oceanic crust, so the continental crust rise above the oceanic crust. Continental crust is broadly **granitic** (**intrusive igneous** rock rich in **quartz** and **feldspar**). $\bar{d} \sim 30 \text{ km}$

Mantle:

Ultrabasic (**ultramafic**) and **mafic** composition. Two major and one minor constituent minerals of the lower mantle are ([Ringwood, 1982](#)):

- Aluminous silicate perovskite [$\text{Al}-(\text{Mg}, \text{Fe})\text{SiO}_3$] 62% (volumetrically)
- Ferropericlase [$(\text{Mg}, \text{Fe})\text{O}$] 33%
- Calcium silicate perovskite (CaSiO_3) 5%

The Structure of the Earth

Basalt: **Aphanitic extrusive** igneous rock (90% of all volcanic rock on Earth) – formed from the **rapid cooling** of mafic lava at the surface or near surface. Because of rapid cooling the sizes of crystals are small.

Granite: Coarse- or medium-grained **intrusive** igneous rock rich in **quartz** and **feldspar** - the most common plutonic rock of the Earth's crust, forming by the cooling of magma (silicate melt) **at depth**.

Rhyolite: A felsic **extrusive** rock – **rich in silica** – **highly viscous**.

Quartz: Silicon dioxide (SiO_2) with minor impurities such as lithium, sodium, potassium, and titanium.

Feldspars: A group of rocks containing aluminum bearing minerals, with elements such as sodium, calcium, potassium or barium. Crystallized from magma as **intrusive** or **extrusive** igneous rock.

Potassium feldspar: (K-spar) endmember KAlSi_3O_8

Albite endmember: $\text{NaAlSi}_3\text{O}_8$

Anorthite endmember: $\text{CaAl}_2\text{Si}_2\text{O}_8$

The Structure of the Earth

Intrusive rock (Plutonic rock): Igneous rock formed from magma forced into older rocks at depths within the Earth's crust. Crystallization by slow solidification at depth – exposed to the surface by erosion.

Extrusive rock: Derived from magma ejected at Earth's surface. They are formed by fast solidification at the surface and have different texture and mineral composition than intrusive rocks.

Aphanites (Aphanitic rocks): Igneous rocks having **fine-grained** components (their component mineral crystals not visible to the naked eye)

Phanerite (Phaneritic rocks): Igneous rock with large visually distinguishable crystals – cooled slowly from magma at deep underground in plutonic environment.

Plutonic: Relating to rock formation by solidification depth.

The Structure of the Earth

Ultramafic rock: (SiO_2 : <45%)

Mafic rock: Rich in **magnesium** and **iron** (SiO_2 : 45%-52%)

Intermediate rock: (SiO_2 : 52%-66%)

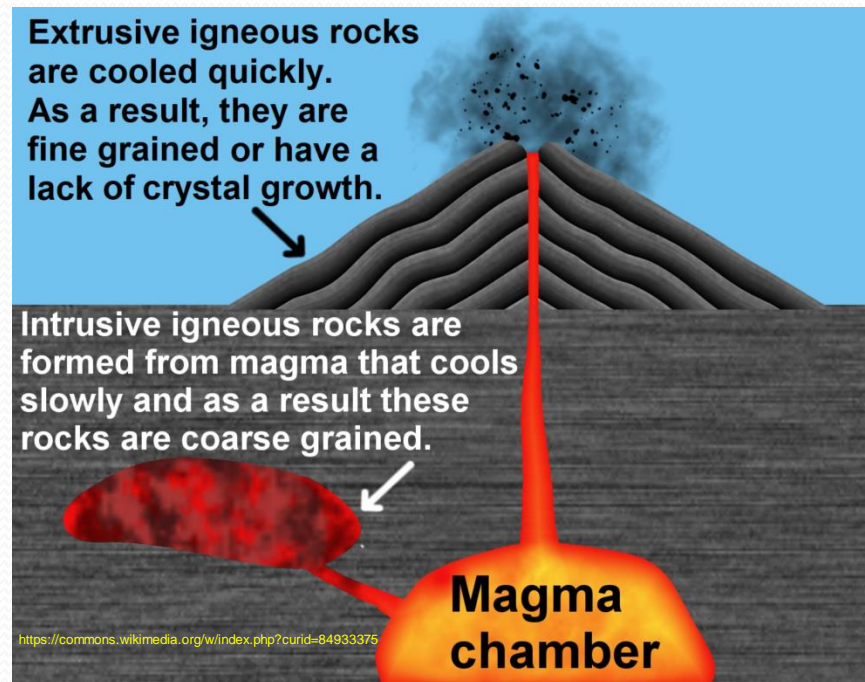
Silicic rock: Rich in **silica** – (e.g., granite and rhyolite) (SiO_2 - > 66%)

Felsic rock: Rich in **feldspar** and **quartz** – enriched in the **lighter** elements such as silicon, oxygen, aluminum, sodium, and potassium – felsic magma/lava has **higher viscosity** than mafic magma/lava (**e.g., granite, rhyolite**).

Silicic rock ~ Felsic rock

Melt forms by:

- Decrease in pressure
- Increase in temperature
- Change in composition



Major Divisions of the Earth

Region	Depth Range (km)	Mass (10^{21} kg)	Mass Fraction (%)	Average Density (kg m^{-3})
Oceanic crust	0–6	6	0.1	3,000
Continental crust	0–30	19	0.3	2,700
Upper mantle	(6,30)–410	615	10.3	3,350
Transition zone	410–660	415	7.0	3,860
Lower mantle	660–2,886	2,955	49.6	4,870
Outer core	2,886–5,140	1,867	31.1	11,000
Inner core	5,140–6,371	98	1.6	12,950
Whole Earth	0–6, 371	5,975	100	5,515

Bulk Earth Composition

Element	Mantle wt (%)	Core wt (%)	Bulk Earth wt (%)
Al	2.35		1.59
Ca	2.53		1.71
Mg	22.8		15.4
Si	21.0		14.2
Fe	6.26	87.5	32.7
Cr	0.263	0.95	0.49
Ni	0.196	5.40	1.89
Mn	0.105	0.50	0.24
Na (ppm)	2,670		1,800
V (ppm)	82	120	95
Co	0.0105	0.26	0.0915
P	0.009	0.050	0.17

McDonough and Sun (1995).

Basic Concepts of Thermodynamics

Reversible process: In thermodynamics, a reversible process is a process **whose direction can be "reversed"** by inducing infinitesimal changes to some property of the system via its surroundings. It is a quasi-static process where no dissipative forces such as friction forces are present. For reversible process we have:

$$\Delta S = 0 \text{ (entropy)}$$

$$\delta w = -PdV$$

$$\delta Q = TdS$$

Adiabatic process: A process occurs **without heat or mass transfer** between a thermodynamic system and its surroundings and energy is transferred to the surroundings only as work.

$$\Delta Q = 0$$

$$\Delta m = 0$$

Isentropic process: An idealized thermodynamic process that is both **adiabatic** and **reversible**. The work done to the system or taken out is frictionless and non-dissipative, and there is not net mass transfer of heat or mass. During this process entropy doesn't change:

$$\Delta S = 0$$

$$\delta w = -PdV$$

$$\delta Q = TdS$$

$$\Delta Q = 0$$

$$\Delta m = 0$$

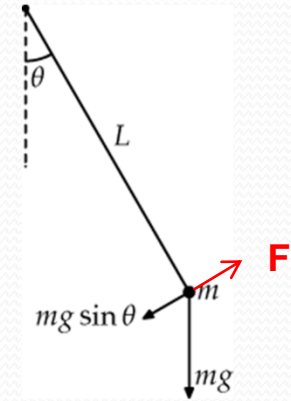
Basic Concepts of Thermodynamics

Ex. – Reversible process

$$\left\{ \begin{array}{l} F(\theta) = mg \sin \theta \quad \text{Initial state in equilibrium} \\ F(\theta) + F = 0 \end{array} \right.$$

$$F \rightarrow F' \left\{ \begin{array}{l} F(\theta') = mg \sin \theta' \quad \text{Perturbed state in equilibrium} \quad F' = F + \epsilon \\ F(\theta') + F' = 0 \end{array} \right.$$

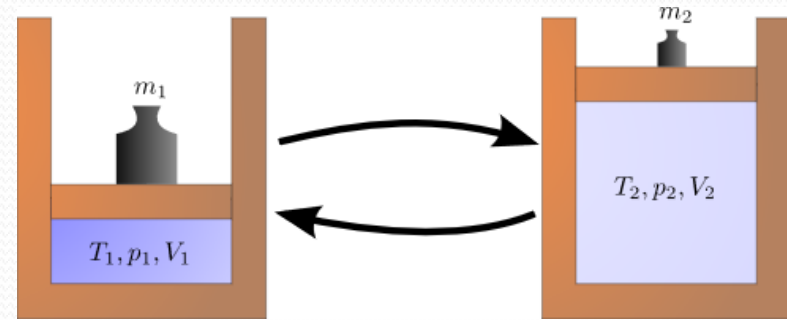
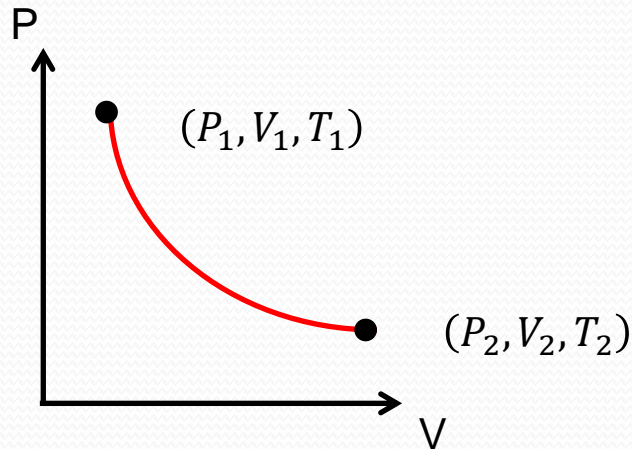
$$F' \rightarrow F \left\{ \begin{array}{l} F(\theta) = mg \sin \theta \quad \text{Reversed to the initial state (in equilibrium)} \\ F(\theta) + F = 0 \end{array} \right.$$



No friction

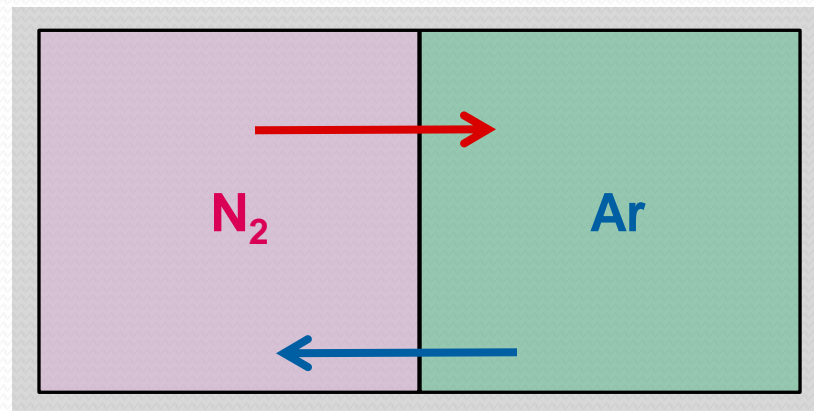
Basic Concepts of Thermodynamics

Ex. – Reversible adiabatic process - Compression or expansion



No heat exchange

Ex. – Irreversible adiabatic process –



No heat exchange

Basic Concepts of Thermodynamics

Entropy: Entropy is a measurable physical property, a measure of the state of disorder, randomness, or uncertainty.

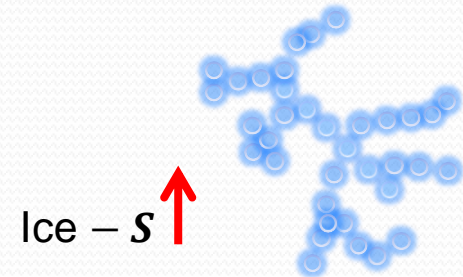
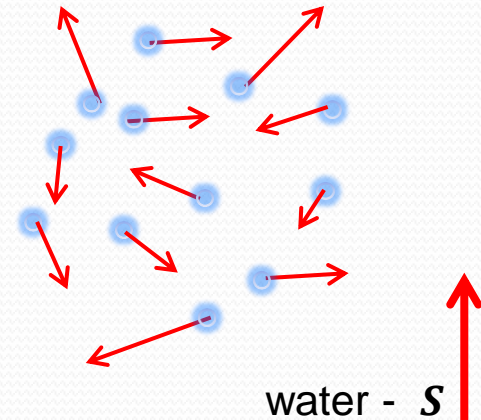
$$dQ = T dS$$

Change in Heat Temperature Change in Entropy

$$\Delta S = S_f - S_i = \int_i^f \frac{dQ}{T} \quad \oint \frac{dQ}{T} = 0 \quad (\text{for reversible process})$$

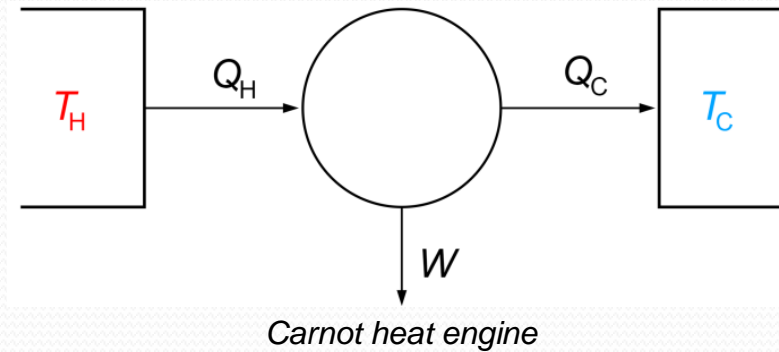
Entropy is a measure of:

- a) Order (higher values \rightarrow system goes to disorder)
- b) Availability of work



Basic Concepts of Thermodynamics

Heat Death



$$T_H \rightarrow T_C \quad \longrightarrow \quad W \rightarrow 0$$

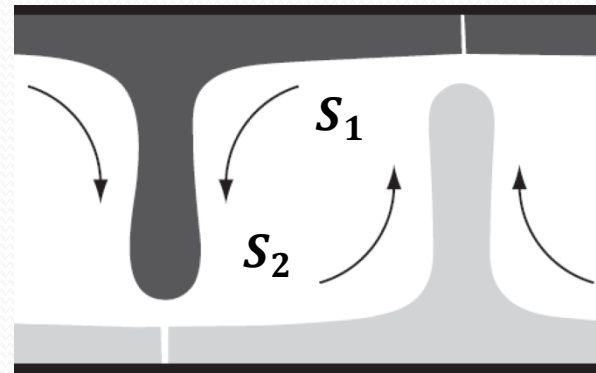
Basic Concepts of Thermodynamics

The Mantle Adiabats :

Suppose a pack of hot mantle material from deep mantle at high pressure is brought to the surface without allowing it to exchange heat with the surrounding mantle material. As pressure decreases (from the deep mantle to the surface), the volume of the pack expands, resulting decrease in density and temperature. The change in temperature as a function of depth is the adiabatic gradient.

$$\frac{dT}{dr} = -(0.4 - 0.5) \frac{K}{km} \quad (\text{upper mantle})$$

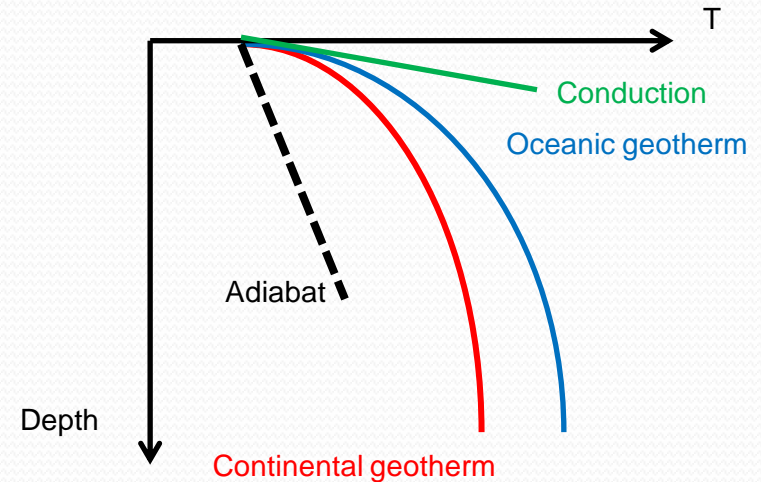
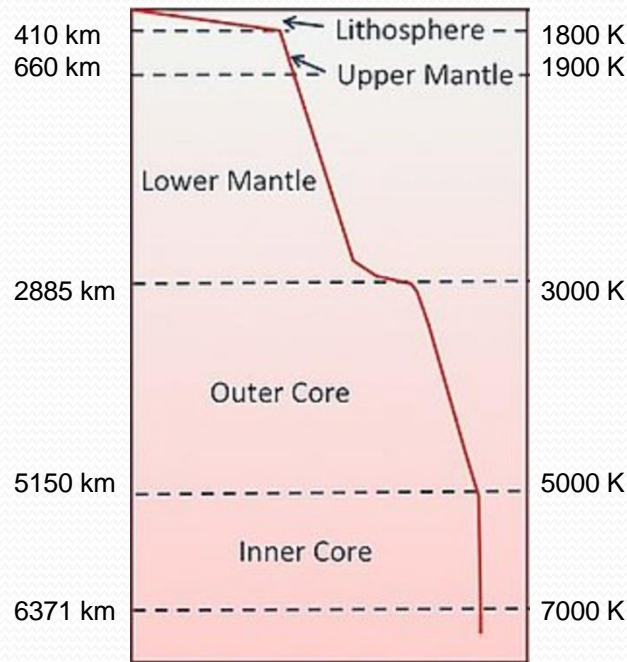
$$\frac{dT}{dr} = -0.3 \frac{K}{km} \quad (\text{lower mantle})$$



Basic Concepts of Thermodynamics

The Mantle Geotherm - Geothermal gradient is the rate of temperature change with respect to increasing depth in Earth's interior.

If the geotherm falls below the adiabat, the convection cannot occur and the heat is transferred by only conduction.



Spherically Averaged Earth Structure

Mantle Density

Equation of state for describing compressibility in chemically homogeneous layers
(**Williamson and Adams**)

$$\frac{d\rho}{dr} = \left(\frac{\partial\rho}{\partial P}\right)_S \frac{dP}{dr} + \left(\frac{\partial\rho}{\partial S}\right)_P \frac{dS}{dr}$$

but

$$\kappa_a = \frac{1}{\rho} \left(\frac{\partial\rho}{\partial P}\right)_S = \frac{1}{K_a} \quad \text{adiabatic compressibility}$$

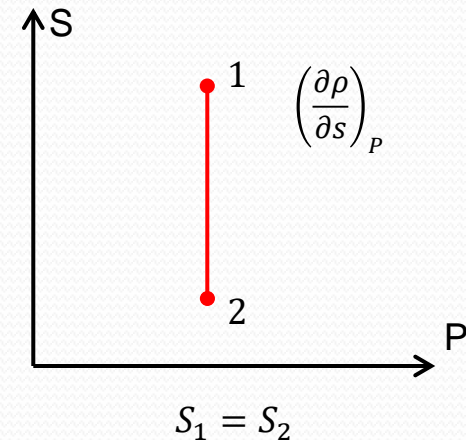
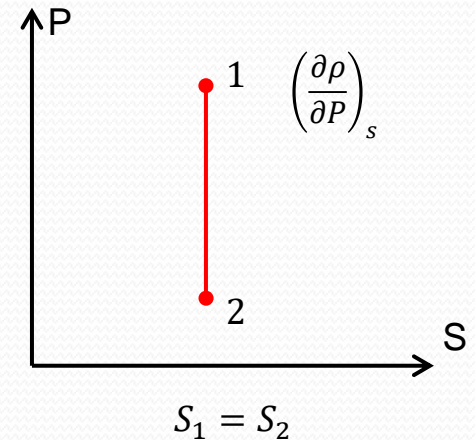
K_a bulk modulus

Also from seismological data

$$\phi = V_P^2 - \frac{4}{3}V_S^2 \equiv \frac{K_a}{\rho} \quad \text{seismic parameter}$$

where

$$V_P = \left(\frac{K_a + 4\mu/3}{\rho}\right)^{1/2}, \quad V_S = \left(\frac{\mu}{\rho}\right)^{1/2}$$



Spherically Averaged Earth Structure

From the definition of the bulk modulus

$$\left(\frac{\partial \rho}{\partial P}\right)_s = \frac{\rho}{K_a} \quad \longrightarrow \quad \left(\frac{\partial \rho}{\partial P}\right)_s = \frac{1}{\phi}$$

- The radial profiles of V_P and V_S are determined from **seismology**.
- For a **homogeneous layer that is well mixed**, e.g., by convection, it is appropriate to assume that the layer is isentropic ($\frac{ds}{dr} = 0$).

$$\frac{d\rho}{dr} = \left(\frac{\partial \rho}{\partial P}\right)_s \frac{dP}{dr} + \cancel{\left(\frac{\partial \rho}{\partial s}\right)_P} \frac{ds}{dr} \quad \longrightarrow \quad \frac{d\rho}{dr} = \frac{1}{\phi} \frac{dP}{dr}$$

For adiabatic compression

$$\frac{dP}{dr} = -\rho g(r) \quad \longrightarrow \quad \frac{d\rho(r)}{dr} = -\frac{\rho(r)g(r)}{\phi(r)}$$

Spherically Averaged Earth Structure

This result is valid only if the **composition is uniform**. For a spherically symmetric Earth model $g(r)$ satisfies the Poisson equation:

$$\frac{1}{r^2} \frac{d}{dr} (r^2 g(r)) = 4\pi G \rho$$

G : Gravitational const.

Boundary conditions.:
Earth's mass,
Earth's moment of inertia

$$\frac{d\rho(r)}{dr} = - \frac{\rho(r)g(r)}{\phi(r)}$$

$$\frac{1}{r^2} \frac{d}{dr} (r^2 g(r)) = 4\pi G \rho$$

$$\frac{dm}{dr} = 4\pi r^2 \rho(r)$$

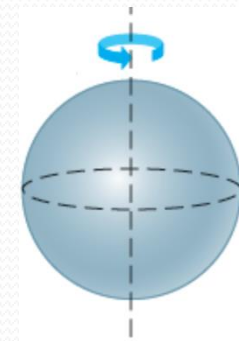
$$\frac{dP}{dr} = -\rho(r)g(r)$$

$$I = \sum_{i=1}^N m_i r_i^2$$

$$I = \int_0^M r^2 dm$$

$\rho(r)$
 $g(r)$
 $\mu(r)$
 $K_a(r)$

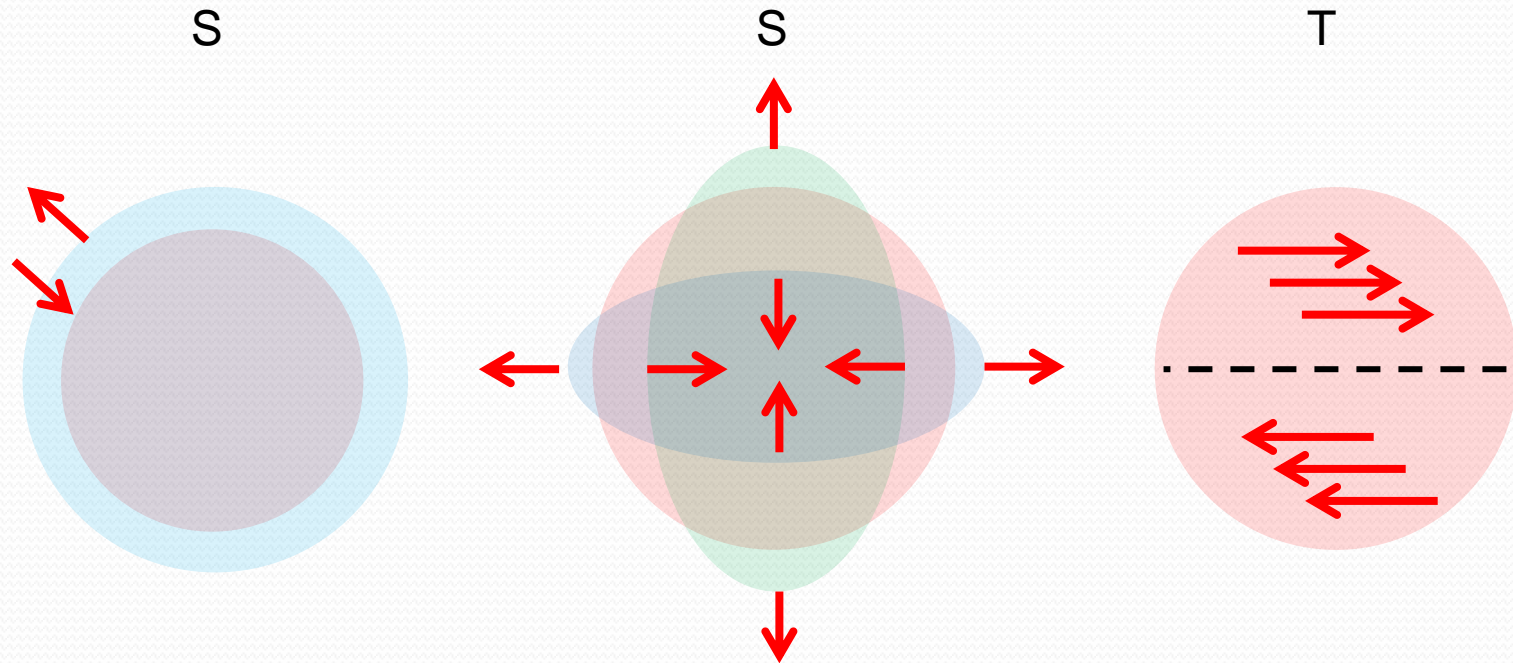
Earth model



Bullen's Earth Model B

Normal modes

A normal mode of an oscillating system is a pattern of motion in which all parts of the system move sinusoidally with the same frequency and with a fixed phase relation. The normal modes of Earth are of two types, **spheroidal** and **toroidal**. They can be used to explore the gross properties of the Earth (**density, seismic velocities**).



Bullen's Earth Model A

Bullen (1936, 1940) first used the above procedure to obtain a **six-layer Earth model**, consisting of:

Layer A

The crust, from the Earth's surface to the **Moho** (at a mean depth of 6 km beneath the oceans and 30km beneath the continents),

Layer B

An adiabatic upper mantle, from the **Moho** to a depth of 400 km,

Layer C ???

From 400km depth to 1,000 km depth.

Layer D

An adiabatic lower mantle, from a depth of 1,000km to a depth of 2,900 km,

Layer E

An adiabatic outer core, from a depth of 2,900km to 5,100 km,

Layer F

An adiabatic inner core, from 5,100km depth to the center of the Earth.



He found that the adiabatic approximation **was not appropriate** for the transition zone (**layer C**), from a depth of 400km to 1,000 km, and instead used **a polynomial function of radius** to represent the density variation in this layer.

Bullen's Earth Model B

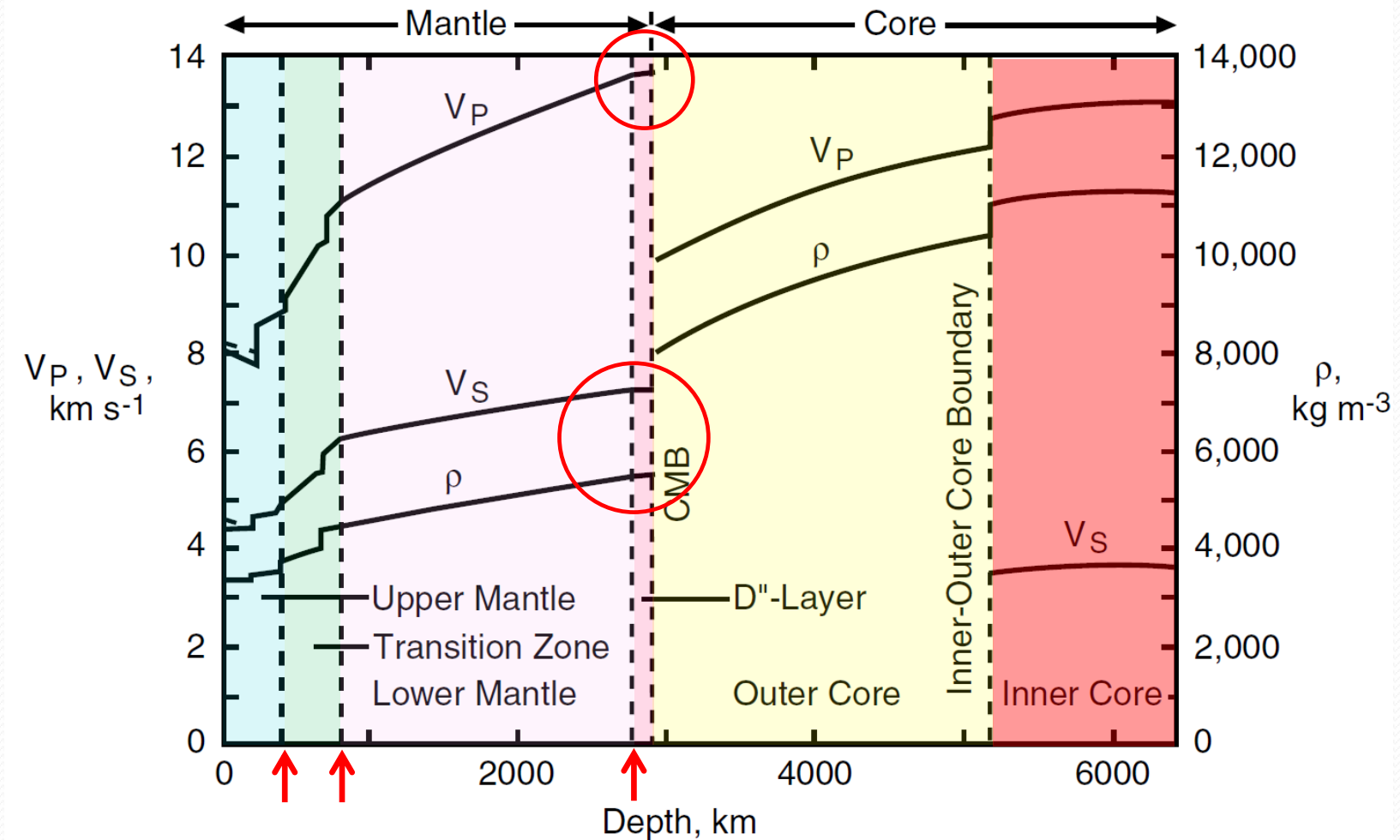
Later, **Bullen** published **model B**, in which he added the assumption of **continuity in the bulk modulus and its pressure derivative** across the **core–mantle boundary**. This allowed him to further subdivide the lower mantle into **layers D**, to a depth of 2,700 km, and **D**, between 2,700km and 2,900km depth.

PREM Model

Spherically symmetric Earth models such as Dziewonski and Anderson's **1981 Preliminary Reference Earth Model (PREM)** are derived **using P-wave** (compressional wave) and **S-wave** (shear wave) travel times and **normal mode** frequencies. The technique used to determine the average density in each layer of the model.

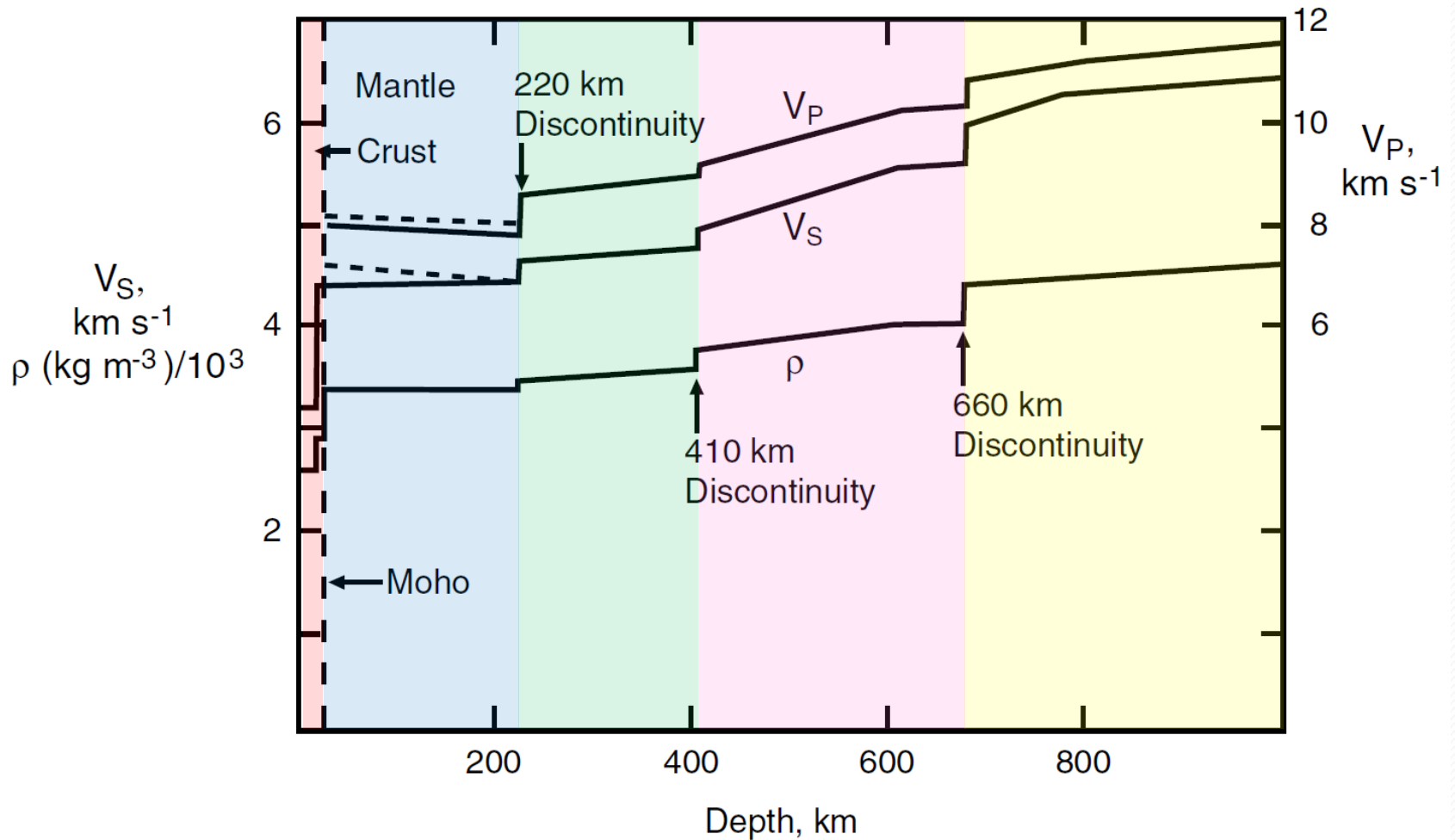
PREM Earth Model

Preliminary Reference Earth Model



Spherical Earth model PREM (Dziewonski and Anderson, 1981). The seismic velocities V_P , V_S and density ρ are given as a function of depth.

PREM Earth Model



Structure of the upper mantle from the spherical Earth model PREM (Dziewonski and Anderson, 1981).

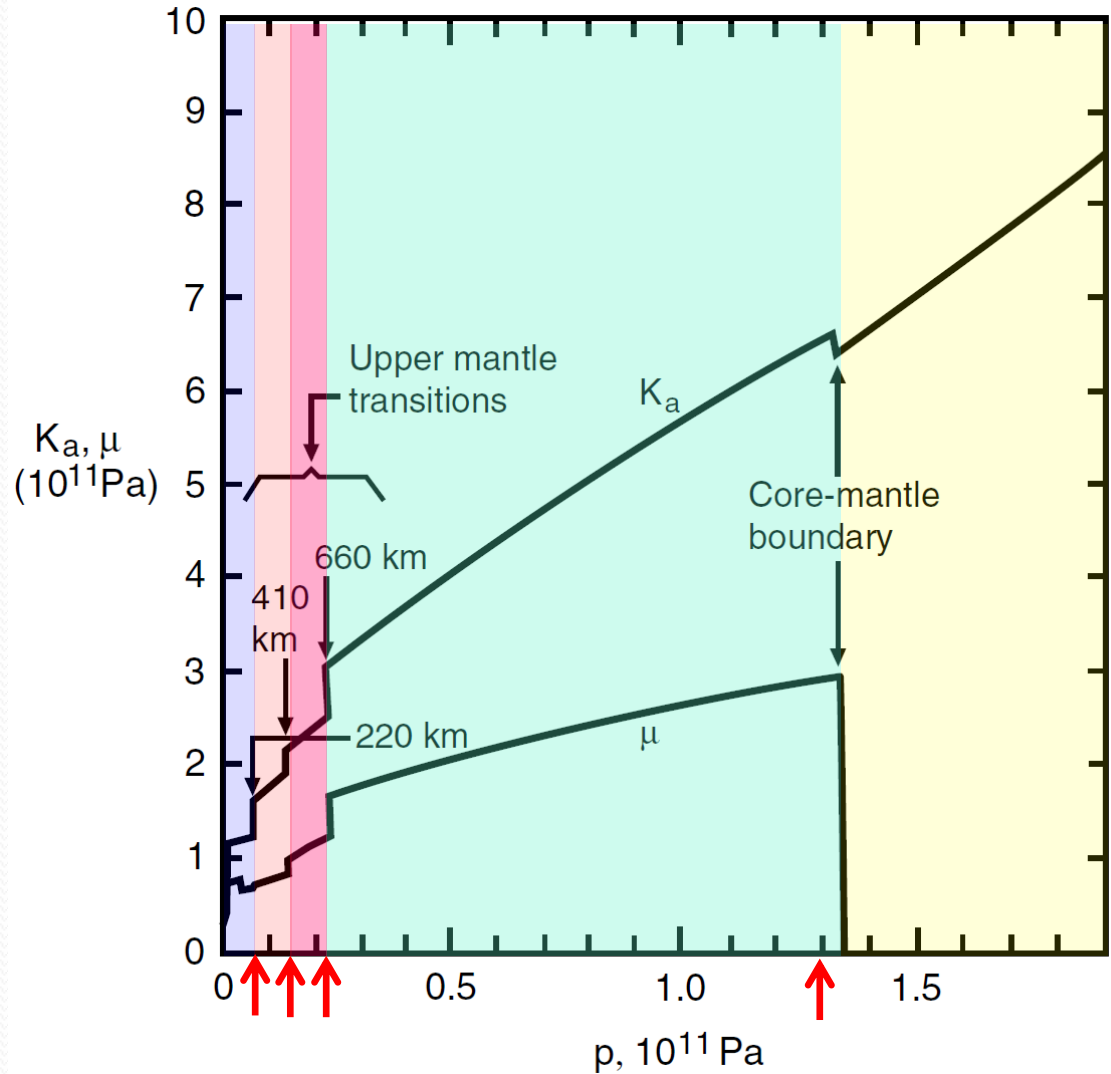
PREM Earth Model

220 km depth: Lehmann discontinuity, it appears beneath continents but not usually beneath oceans. May reflect local anisotropy due to **shearing** of the asthenosphere, or a phase transition. Although present on PREM, it is now generally accepted not to be a global feature.

410 km depth: Exothermic phase transition, β –spinel to γ –spinel.

660 km depth: Endothermic phase transition γ –spinel to perovskite (Pv).

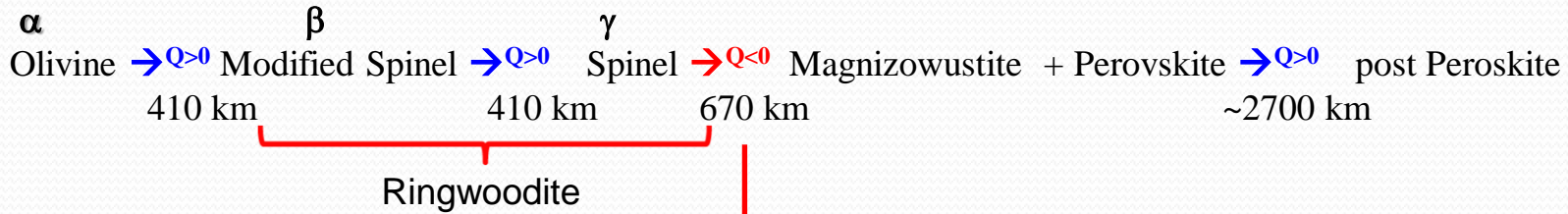
2700 km depth: Exothermic phase transition, perovskite to post-perovskite (Pv-pPv).



Dependences of the Earth's adiabatic bulk modulus K_a and shear modulus or rigidity μ on pressure in the spherical Earth model PREM (Dziewonski and Anderson, 1981).

Mantle Phase Transitions

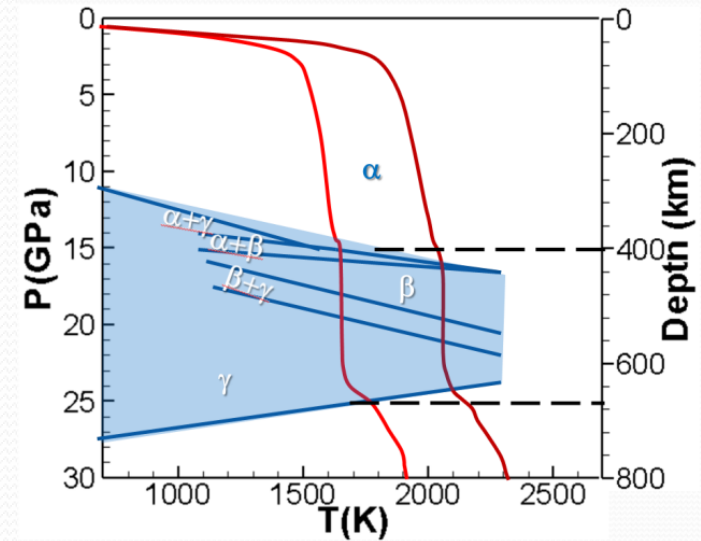
Phase Transitions in Upper Mantle



Additional phase transition (20-30 GPa)

Spinel + Stishovite \rightarrow Ilmenite $\rightarrow Q < 0$ Perovskite
 ~20 GPa ~24 GPa & 800 C

- Olivine, Modified Spinel, Spinel: $(Mg_x, Fe_{1-x})_2SiO_4$
- Magnesiowüstite: $(Mg, Fe)O$
- Perovskite, post-Perovskite: $(Mg, Fe) SiO_3$
- Wüstite: (FeO)
- Periclase: (MgO)
- Stishovite: SiO_2



Schubert et. al, 1975; Akaogo et al., 1989; Solheim & Peltier, 1994

Ferropericlase or **Magnesiowüstite** depending the **fraction** of **Fe** and **Mg**

- Exothermic reaction: Releases heat
- Endothermic reaction: Absorbs heat

Major Constituent Minerals

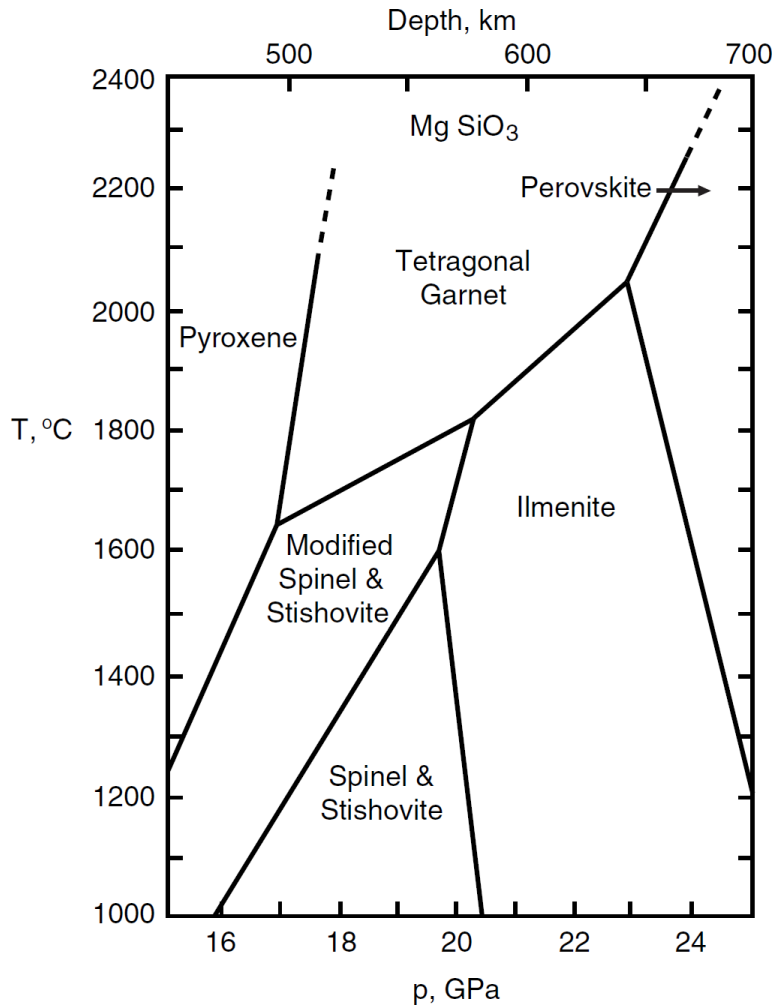
Ringwoodite: $(\text{Mg,Fe})_2\text{SiO}_4$, (γ -phase) an abundant olivine polymorph within the Earth's mantle from about **520 to 660 km** depth, and a rare mineral in meteorites (with the spinel structure). Ringwoodite is the high-pressure polymorph of olivine that is stable at high temperatures and pressures of the Earth's mantle between 525 to 660 km depth. The **discontinuity observed at 520 km** depth may correspond to this phase transition.

Clapeyron slopes and density contrast at the mantle transition zones

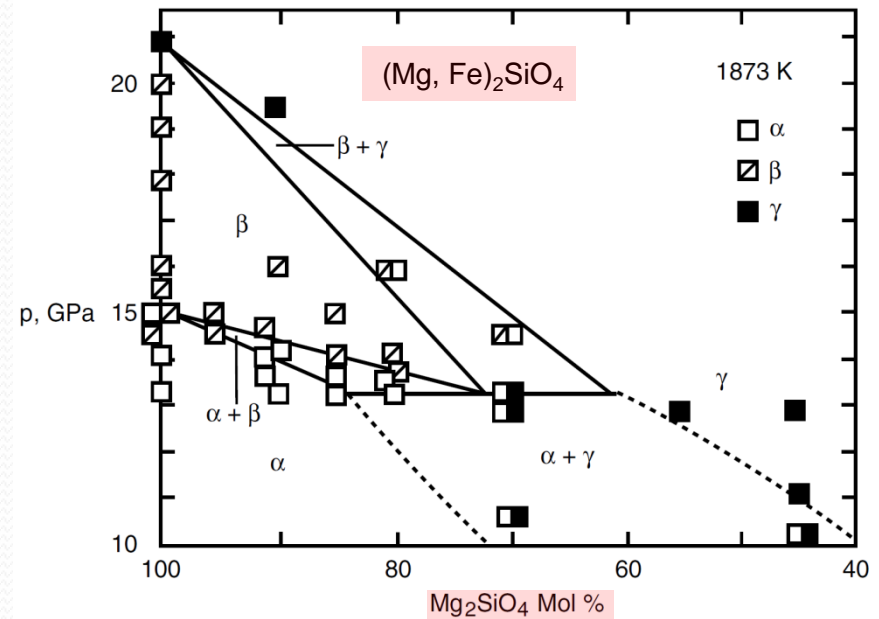
$\gamma_{410} \sim 3 \text{ MPa/K}$	$\Delta\rho = \sim 220 \text{ kg/m}^3$
$\gamma_{660} \sim -3 \text{ MPa/K}$ (Spinel-Perovskite)	$\Delta\rho = \sim 440 \text{ kg/m}^3$
$\gamma_{660} \sim -6 \text{ MPa/K}$ (Spinel + Stishovite \rightarrow Ilmenite \rightarrow Perovskite)	
$\gamma_{2700} \sim 8 - 12 \text{ MPa/K}$	$\Delta\rho = \sim 80 \text{ kg/m}^3$

Broad depth range of transitions in the upper mantle causes gradients in mantle properties rather than single discontinuity.

Phase Diagrams

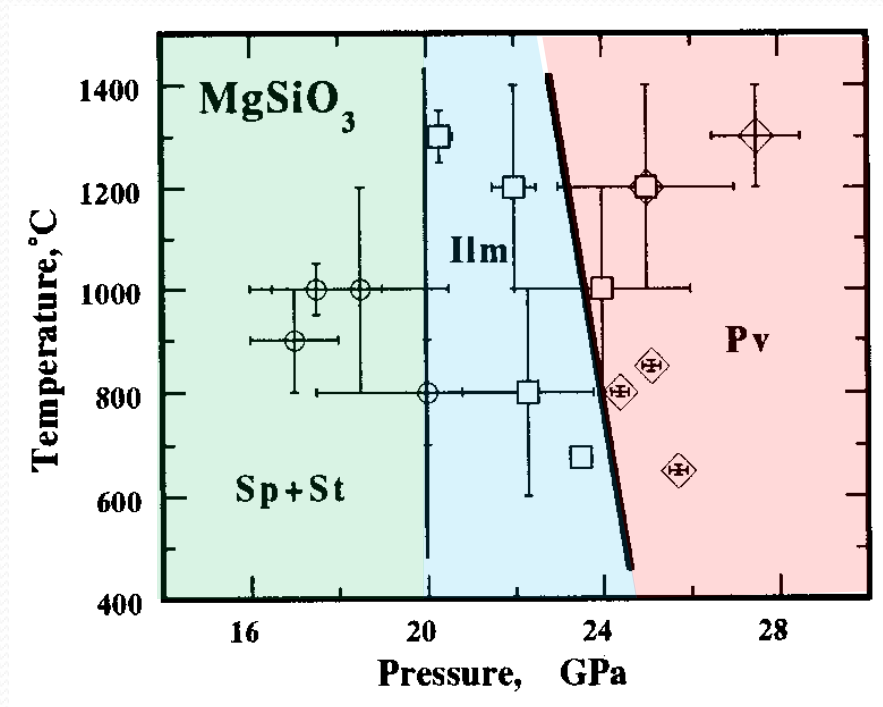


Phase stability fields in temperature–pressure coordinates for MgSiO_3 . After Sawamoto (1987).



Phase diagram for the system $(\text{Mg, Fe})_2\text{SiO}_4$ at pressures of 10–21 GPa and $T = 1,873 \text{ K}$ (Katsura and Ito, 1989).

Mantle Phase Transitions



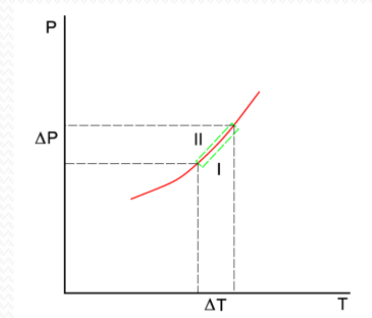
High-pressure phase relations of Mg SiO₃ . Circles , squares and diamonds represent assemblage of Spinel and stishovite, ilmenite and perovskite respectively (Kato et al., 1995). The phase boundaries are represented by solid and bold solid lines.

Mantle Phase Transitions

The Clausius-Clapeyron relation

An equation for a single-component system consisting of two phases in thermodynamic equilibrium at absolute temperature T and pressure P . The relation gives the slope of the coexistence curve in the P - T diagram.

$$\gamma = \frac{dP}{dT} = \frac{l}{Q\Delta V}$$



where l , Q , and ΔV are the latent heat, is the molar heat of transition and the change in volume.

First-order phase transition

A transition that involves a latent heat. During the transition, the system either **absorbs** or **releases** a fixed amount of energy per volume. During this process, the **temperature of the system remains constant**. Second order phase transition is continuous phase transition.

Mantle Phase Transitions

$$C_P \bar{\rho} \frac{DT}{Dt} - \alpha T \frac{DP}{Dt} = \nabla \cdot (K \nabla T) + \phi + \bar{\rho} H + \rho l_i \frac{D\Gamma_i}{Dt} \quad \text{Energy equation}$$

$$\rho = \bar{\rho} \left[1 - \alpha(T - T_r) + \frac{1}{K_T} (P - P_r) \right] + \Delta\rho_i (\Gamma_i - \Gamma_{ri}) \quad i=1,2,3$$

$$\Gamma_i = \frac{1}{2} [1 + \tanh(\pi_i)]$$

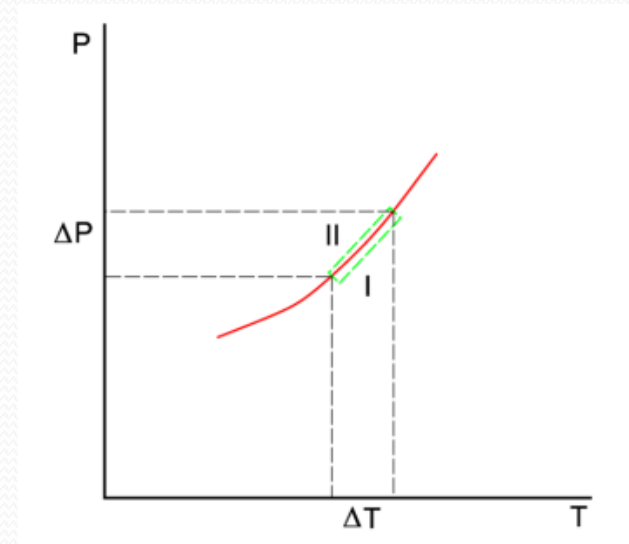
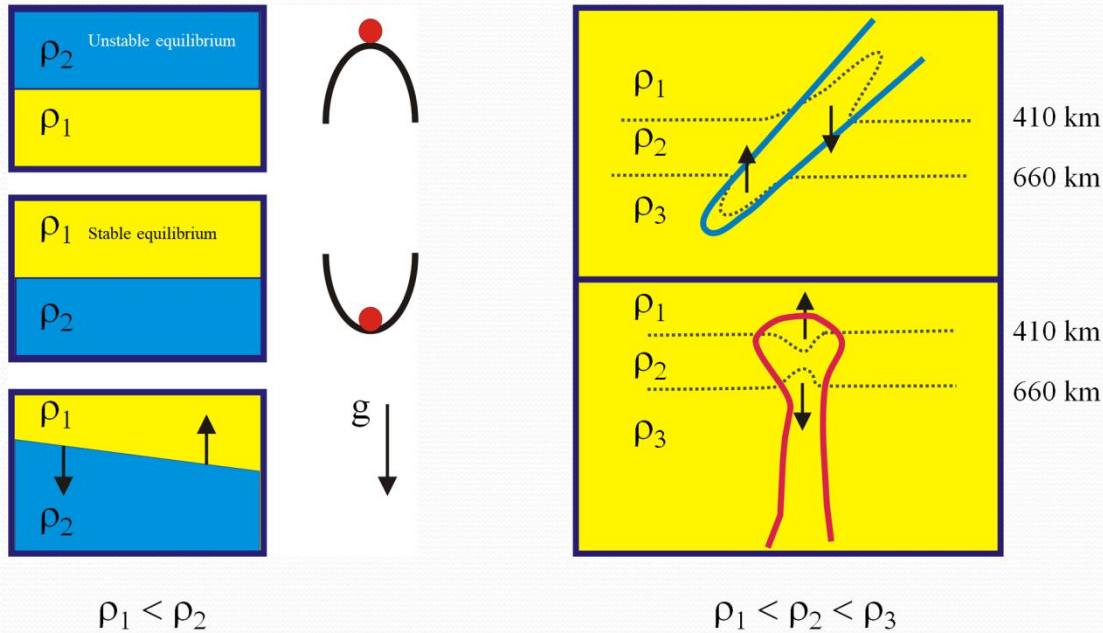
$$\pi_i = \frac{d_i - d - \gamma_i (T - T_i)}{h_i}$$

where d , T , d_i , γ_i , T_i , h_i , and l_i are depth, temperature, reference depth, the Clapeyron slope, transition temperature, the width, and the latent heat of the i^{th} divariant phase transition, respectively.

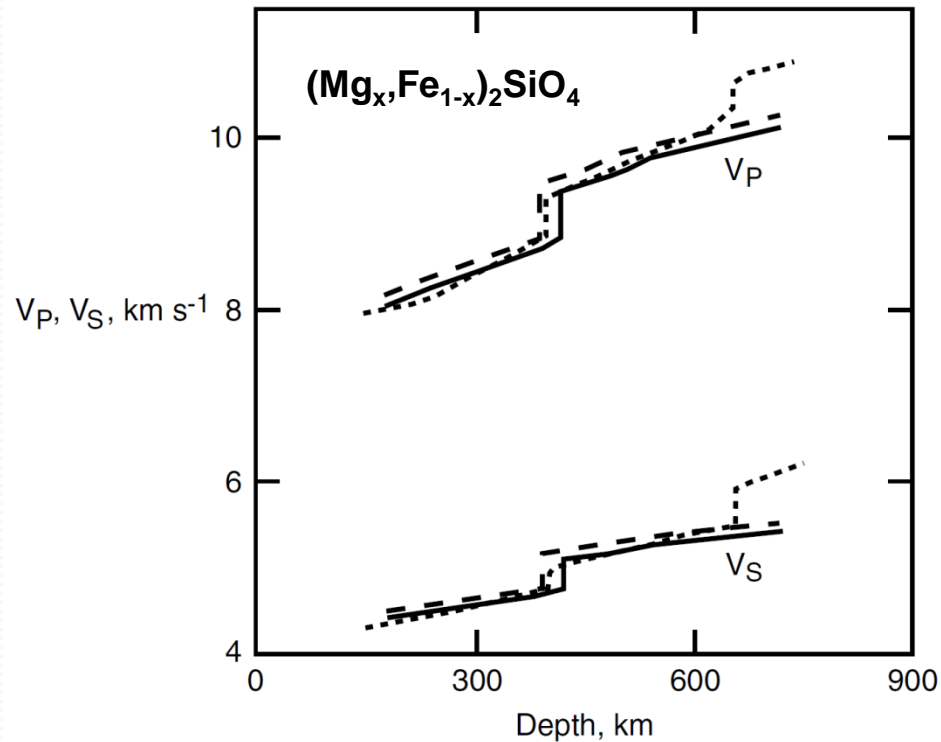
Mantle Phase Transitions

Flow acceleration and deceleration at 410 km and 660 km depth phase transitions

Buoyancy force ~ Lateral variation of density or temperature

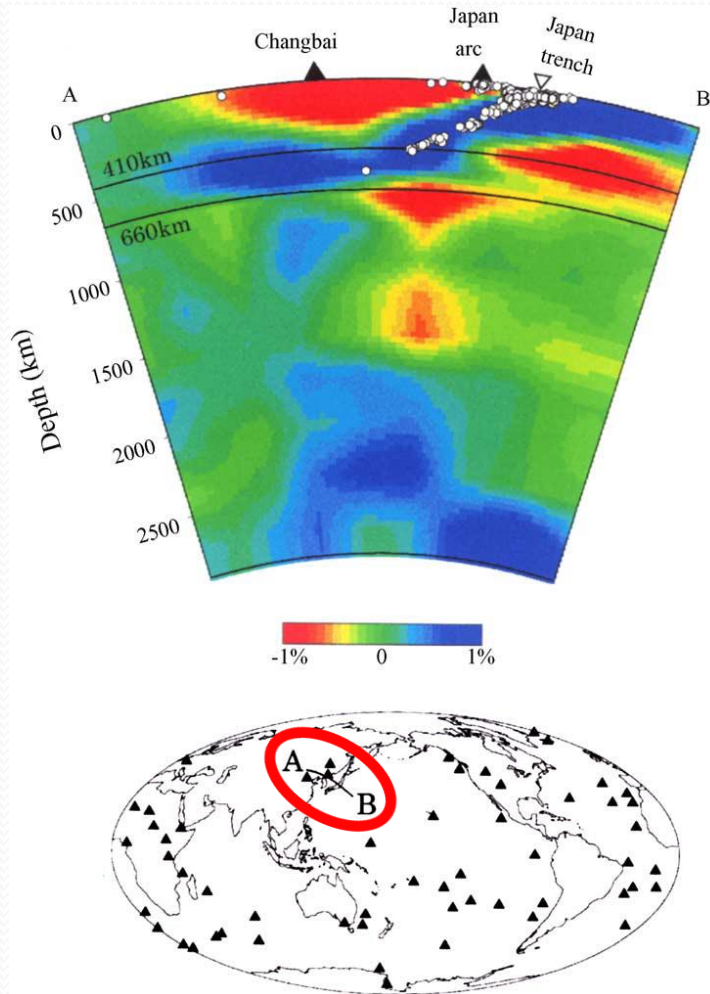


The Transition Zone

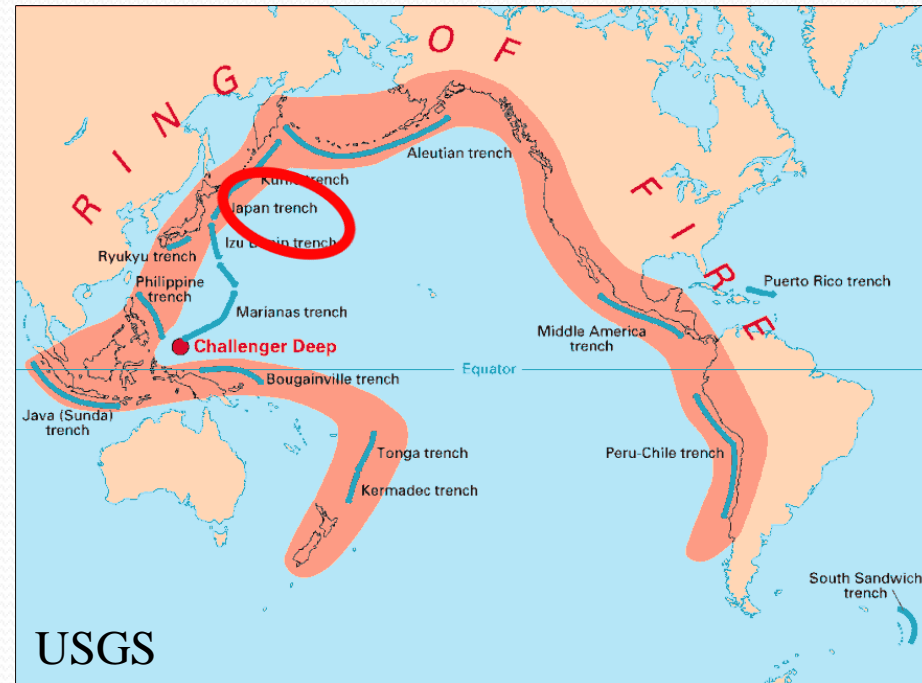


Depth profiles of V_P and V_S in the transition zone given by Bina and Wood (1987) for $x_{\text{Mg}} = 90$ olivine composition along 1,700K (dashed) and 2,000K (solid) isotherms. Dotted curves are the regionalized velocity profiles for North America given by Grand and Helmberger.

Slab Stagnation



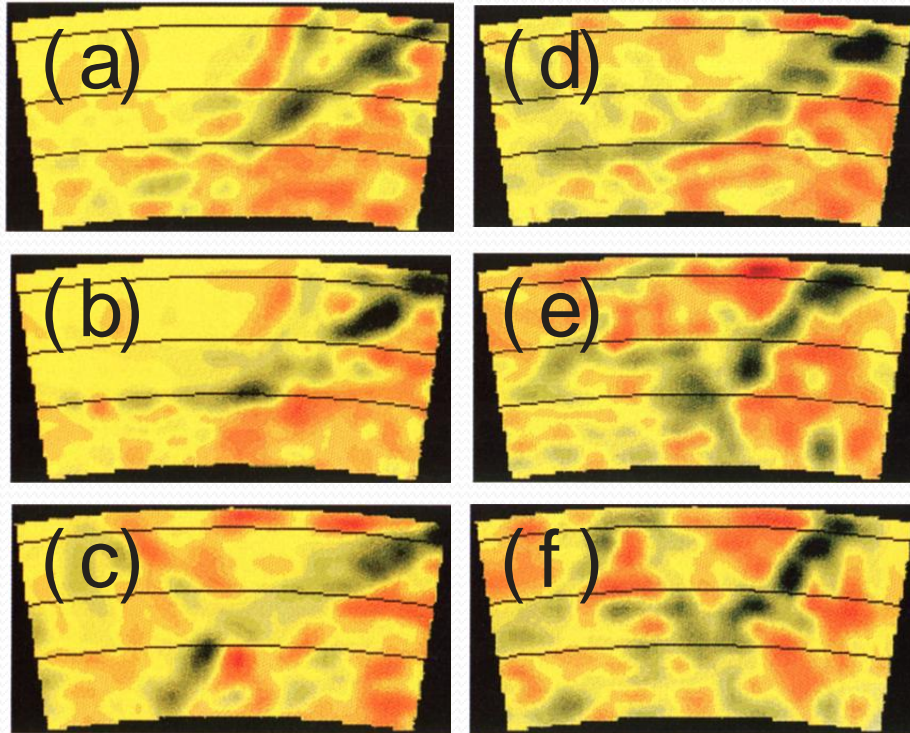
Is the 670 km transition a barrier to whole-mantle convection?



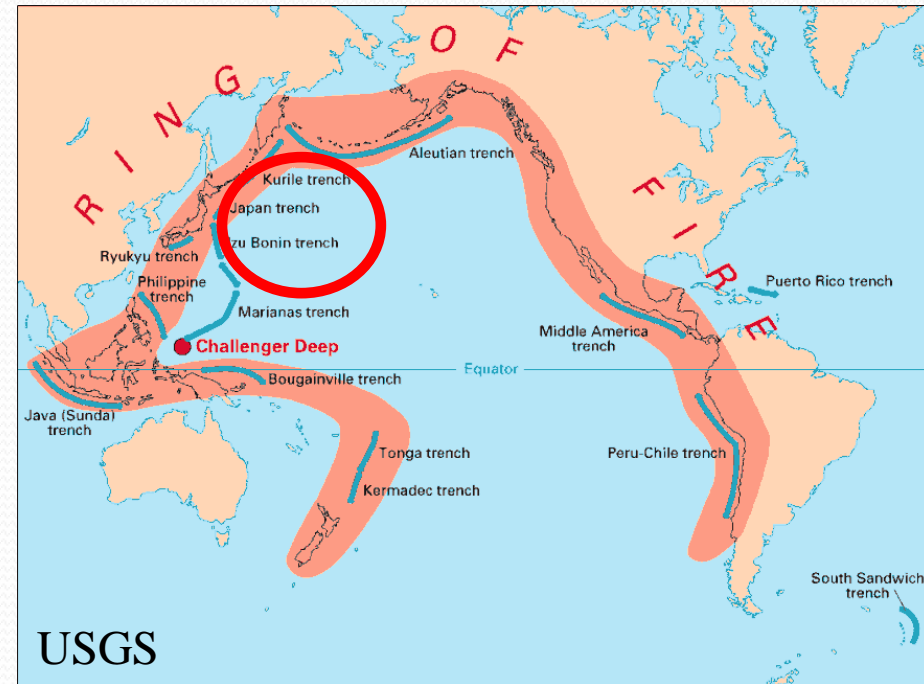
Vertical cross-section of **P-wave anomaly** (Dapeng Zhao, 2004) along a profile passing through **northeast China and central Japan**. White circles denote earthquakes that occurred within a 100-km width from the profile.

Slab Stagnation

P-wave anomalies

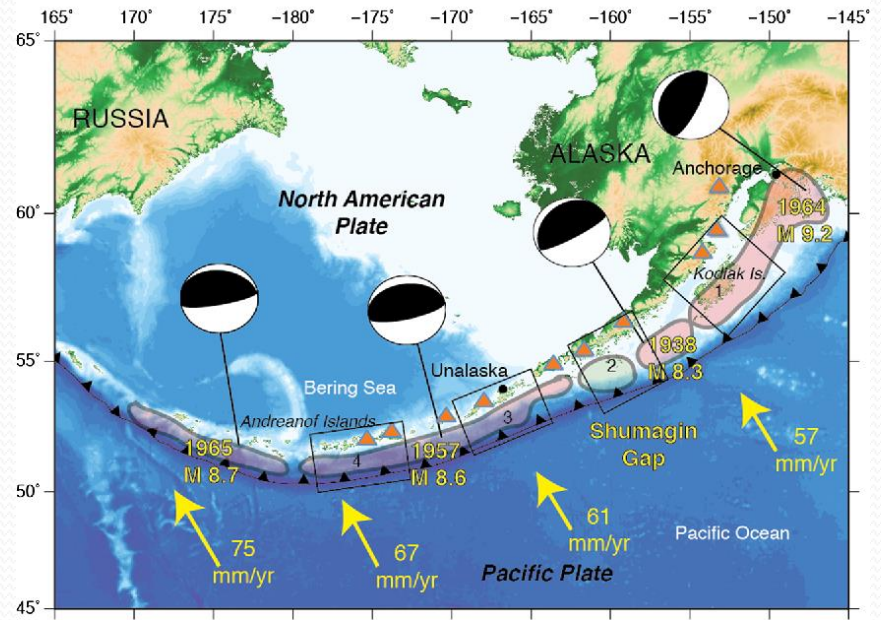
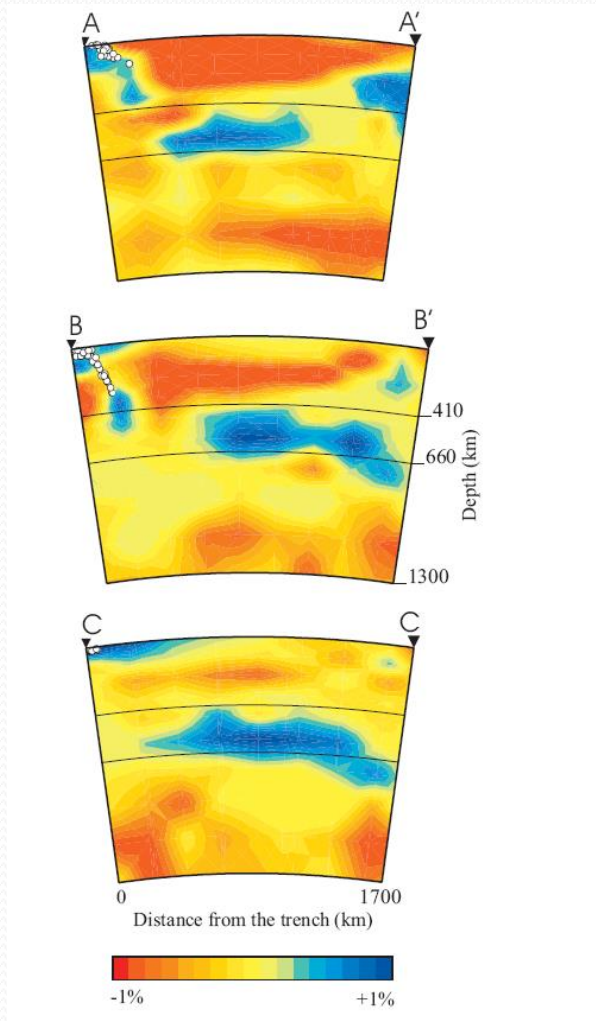


- 3.0%  3.0%



Vertical cross section based on three-dimensional tomographic inversion for the **Kuril slab** (a, b), the **Japan slab** (c, d) and the **Izu slab** (e, f). The depth contours in c-h denote 100, 410, and 660 km depths (Deal and Nolet, 1999).

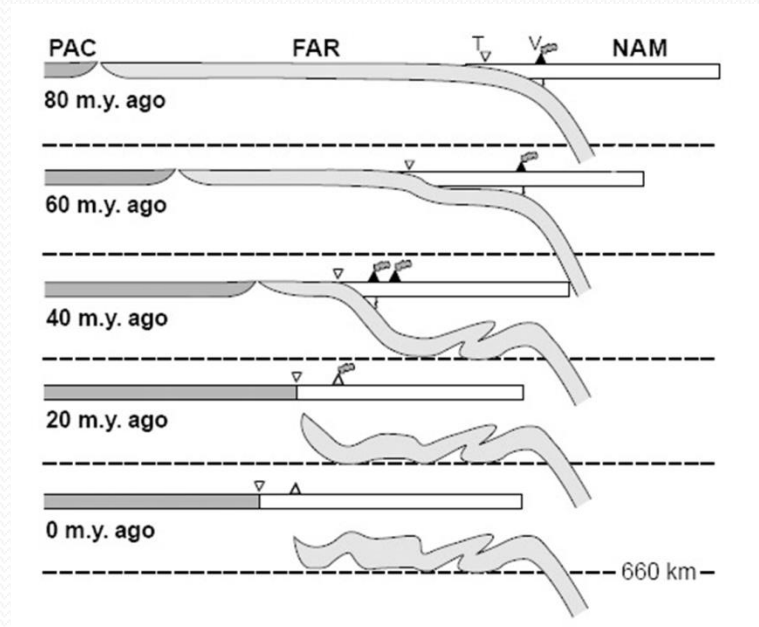
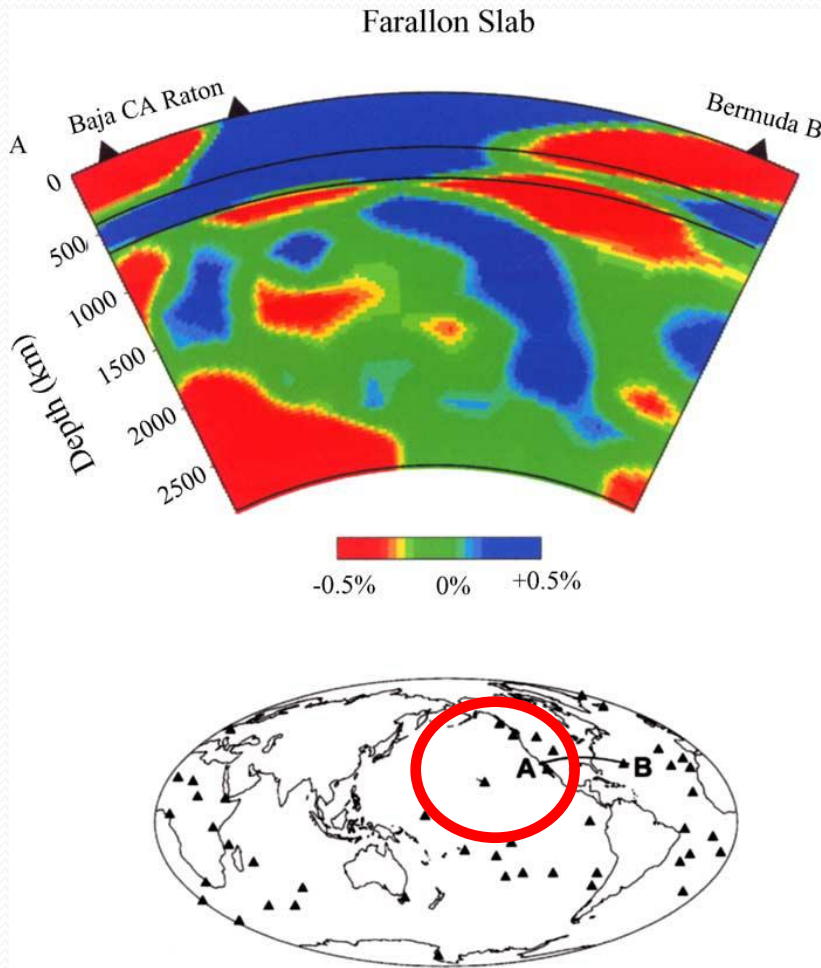
Slab Stagnation



Regional bathymetric/topographic map of the Alaska-Aleutian Subduction Zone (Brown et al, 2013)

Cross-sections of the velocity anomalies along profiles in the **Aleutian subduction zone**. The scale in per cent relative to the reference model ak135 (Kennett et al. 1995; Gorbатов et al., 2000).

Slab Stagnation



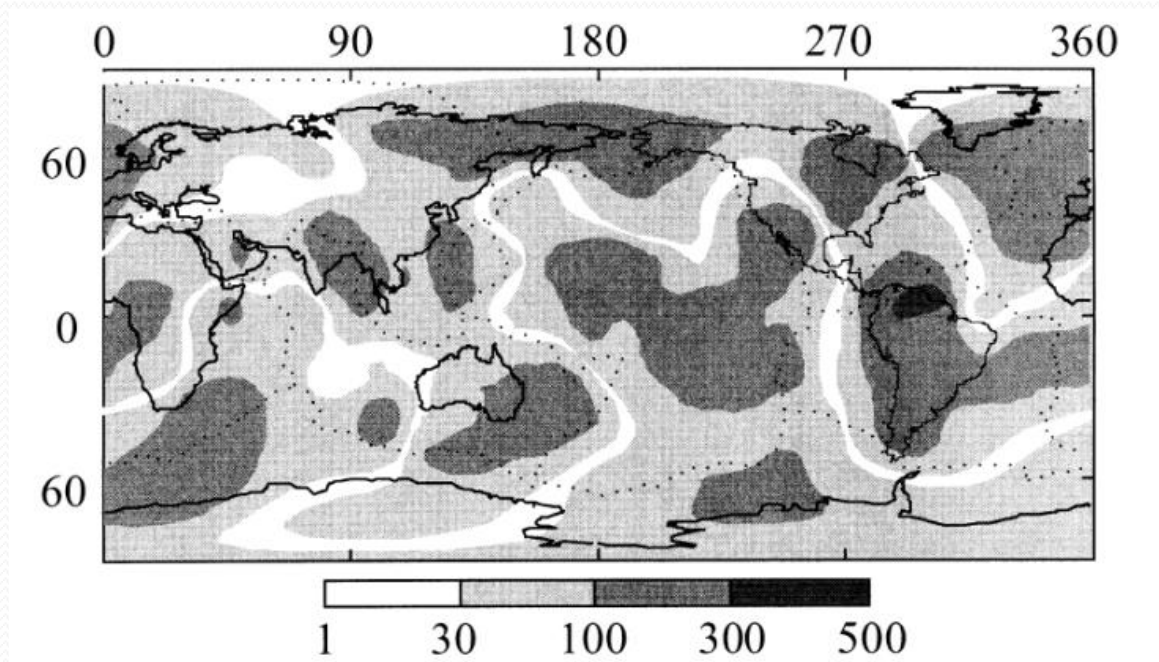
Cartoon of Farallon slab evolution in the upper mantle (Schmid et al., 2002).

Vertical cross-section of P-wave anomaly (Dapeng Zhao, 2004) along a profile passing through **Farallon slab** under southern North America. Solid triangles denote surface hotspots.

Phase Transformational Superplasticity

Superplasticity

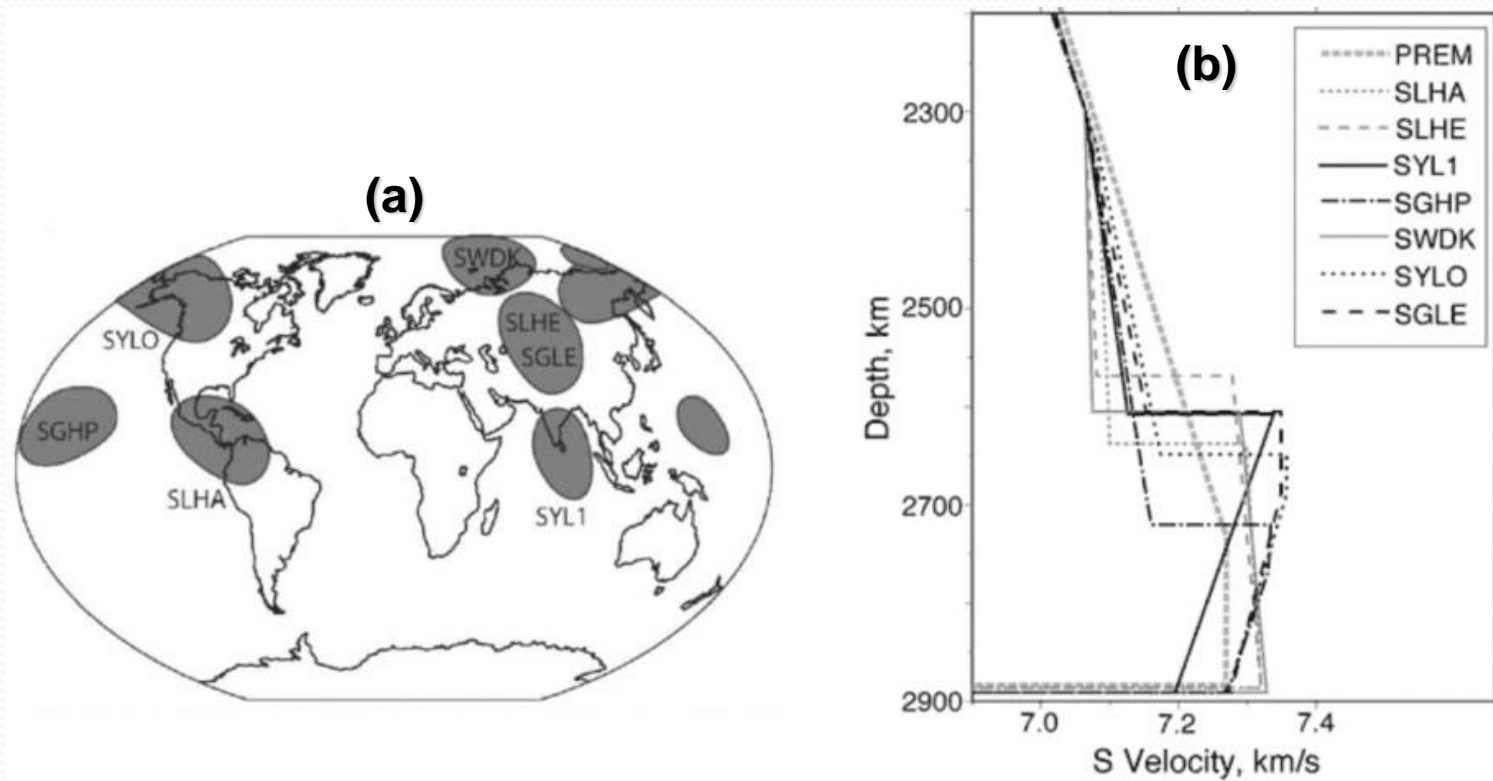
Superplasticity due to the reduction in grain size and/or reduction in cohesion between the atoms during phase transition (e.g. Sammis & Dein, 1974; Paterson, 1983; Ranalli, 1991).



Factor of reduction in viscosity (90 on average)

Transformational superplasticity map at 670 km depth for a mantle flow model with lateral viscosity contrasts inferred from a global seismic tomography model (Svetlana et al., 1998).

Earth Model – Deviations from the PREM



a) Regions where **shear velocity discontinuities** have commonly been observed, with typically a 2–3% increase in velocity at depths ranging from 200 to 300 km above the CMB, b) Radial profiles of shear velocity in the lowermost mantle shown in (a): PREM (Dziewonski and Anderson, 1981), SLHE, SLHA (Lay and Helmberger, 1983), SYL1 (Young and Lay, 1987), SGHP (Garnero et al., 1988), SWDK (Weber and Davis, 1990), SYLO (Young and Lay, 1990), and SGLE (Gaherty and Lay, 1992).

Earth Model – Deviations from the PREM

D''-layer Discontinuity

- a) V_S ←correlated→ V_ϕ (in most of the lower mantle)
- b) V_S ←anti-correlated→ V_ϕ (near the CMB below 2600 km depth)
- c) Increase in ρ and V_S but decrease in V_ϕ (passing D'' level)
- d) Large reduction in V_S and V_P in ULVZ's (5-40 km above the CMB)
- e) Increase in Poisson ratio in ULVZ's

V_S , V_P , V_ϕ : shear, compressional, and bulk velocities

Possible explanations:

1. Thermal
2. Compositional
3. Phase transitional
4. Melt

$$V_\phi = \sqrt{V_P^2 - \frac{4}{3}V_S^2}$$

Earth Model – Deviations from the PREM

- Thermal variation **cannot** reconcile this problem because for pure thermal heterogeneity δV_S and δV_ϕ **would be correlated**.
- Thermal variation alone **cannot** also explain **the high Poisson ratio** for this region.
- Compositional and/or phase transitional solutions are **required**. **Forte & Mitrovica (2001)** argued this problem in terms of the thermal and compositional anomalies.

$$\nu = \frac{\left(\frac{v_P}{v_S}\right)^2}{2\left(\frac{v_P}{v_S}\right)^2 - 2} \quad \text{Poisson ratio}$$

Earth Model – Deviations from the PREM

ULVZs

- Thermal variation alone **can not** reconcile the **large** variability of **shear** velocity in **ULVZs**.
- Partial melting **may** resolve this problem (**Williams & Garnero, 1996**).
- Compositional and/or phase transitional solutions **may** also be part of the explanation.

An alternative explanation

Theoretical calculations show that **S-wave** velocity is **faster** and **bulk-sound** velocity is **slower** in post-perovskite than in perovskite at equivalent pressure (**Hirose & Lay, 2008**).

Earth Model – Deviations from the PREM

New Phase Transition

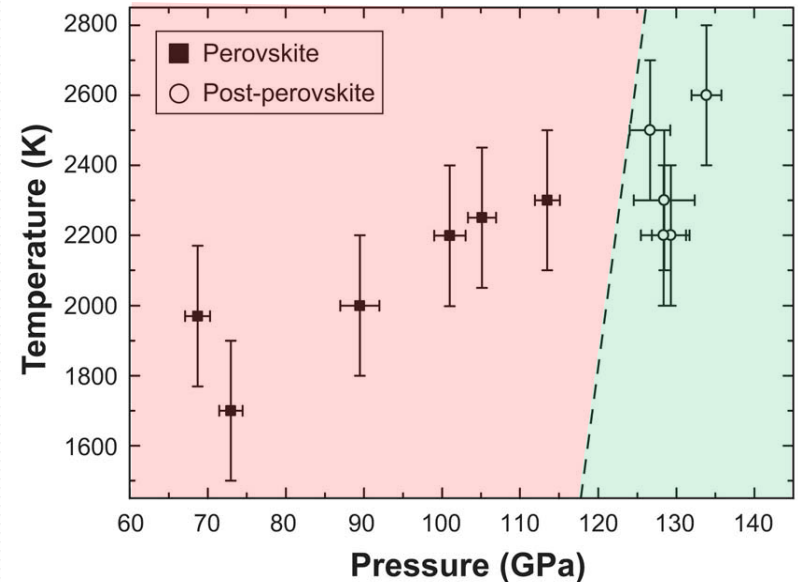
A New Phase Transition

Exothermic phase transition at ~2700 km depth (Pv-pPv)



Evidence

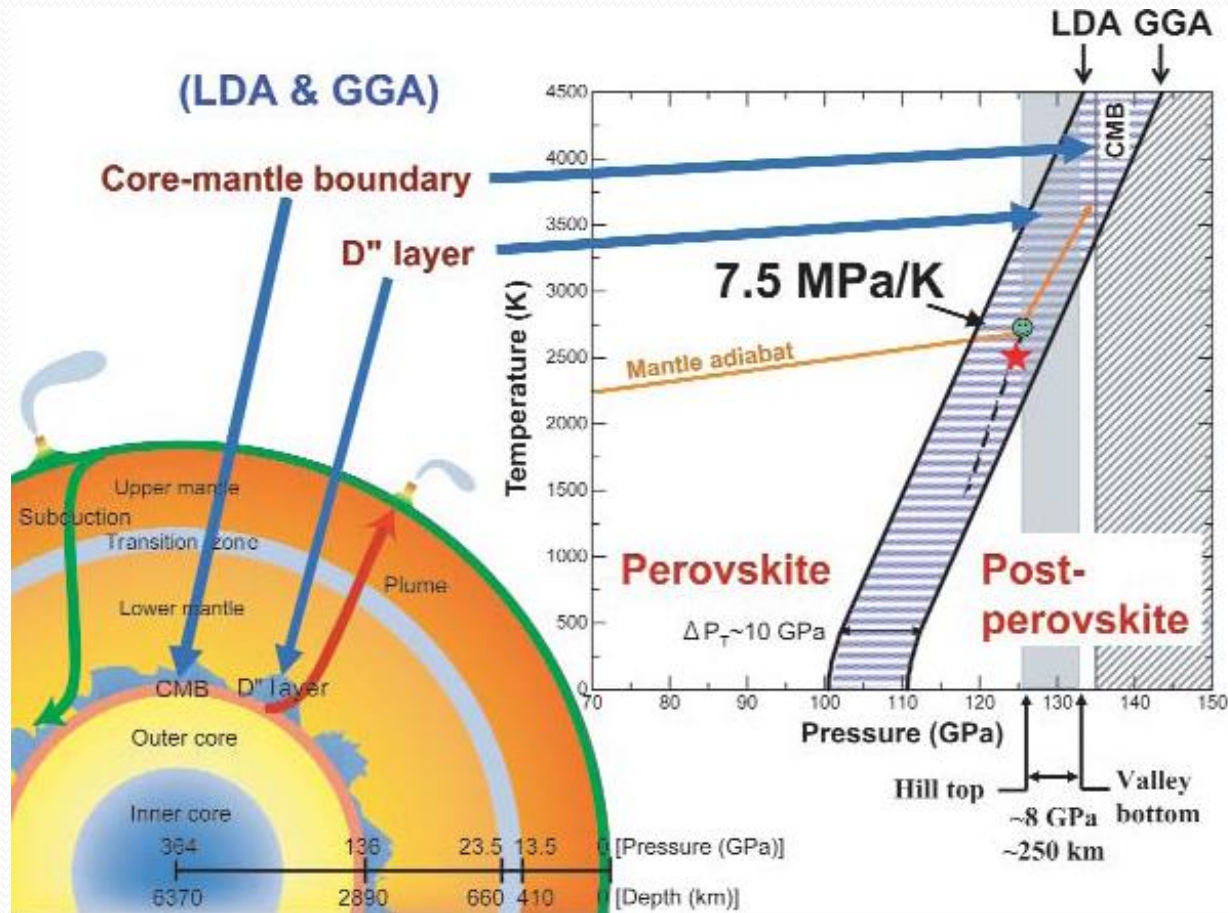
X-ray diffraction measurements of Mg SiO_3 at high pressure and temperature at CMB conditions above 125 GPa and 2500 K (Murakami et al, 2004).



Phase diagram of MgSiO_3 (Murakami et al., 2004). Solid squares and open circles indicate the stabilities of perovskite and post-perovskite phase, respectively. The phase transition boundary proposed by Sidorin *et al.* (1999) is shown by a dashed line.

Earth Model – Deviations from the PREM

New Phase Transition



High P-T phase diagram of MgSiO_3 predicted by first principles calculation based on the local density approximation (LDA) and generalized gradient approximation (GGA) (Tsuchiya et al., 2004). The calculated Clapeyron slope is about 7.5 MPa/K. The vertical shaded bound is the pressure range across the D'' topography. The schematic Earth cross section demonstrates the correspondence of the Earth's structure and the post-perovskite phase transition (Lay et al., 2005).

Earth Model – Deviations from the PREM

New Phase Transition

Theoretical calculations show that **S-wave velocity** is **faster** and **bulk-sound velocity** is **slower** in post-perovskite than in perovskite at equivalent pressure (Hirose & Lay, 2008).

Observation:

Compared to the PREM in ULVZ;

Depression in $V_p \sim 5\%-10\%$

Depression in $V_s \sim 10\%-30\%$

Increase in Poisson's ratio. $\sim 30\%$

	V_p , km/s	V_s , km/s	ν
PREM, mantle side of CMB	13.72	7.26	0.30
ULVZ <small>Thorne & Garnero (2004)</small>	12.35	5.08	0.40
Fs40 ppv at 130 GPa-300 K	12.72	4.86	0.41
Fs40 ppv at 130 GPa-3000 K	11.91	4.05	0.41
	$\sim 13\%$	$\sim 44\%$	$\sim 36\%$

Seismic wave velocities above ULVZ and in ULVZ in comparison to the present Fs40 ppv results (Mao et al., 2006).

Appendix

Basic Concepts of Thermodynamics

Linear Thermal Expansivity

The change in unit length of a solid with temperature at constant tension.

$$\alpha = \frac{1}{L} \left(\frac{\partial L}{\partial T} \right)_f \quad f: \text{tension} \quad (1/\text{K})$$

Volume Thermal Expansivity Coefficient

It is the change in unit volume of a solid, liquid or gas with temperature at constant pressure.

$$\beta = \frac{1}{V} \left(\frac{\partial V}{\partial T} \right)_P \quad \text{isobaric expansivity} \quad (1/\text{K})$$

$$\beta \approx 3\alpha$$

Appendix

Heat Capacity

The amount of heat to be supplied to an object to produce a unit change in its temperature.

$$C = \frac{dQ}{dT}$$

$$c = \frac{1}{m} \frac{dQ}{dT} \quad \text{specific heat (heat capacity per unit mass)}$$

$$C_V = \left(\frac{dQ}{dT} \right)_V \quad C_P = \left(\frac{dQ}{dT} \right)_P \quad (\text{J/K})$$

Appendix

Bulk Modulus

The pressure rise dP per fractional volume decrease $-dV/V$.

$$K = \frac{dP}{-\frac{dV}{V}} = -V \frac{dP}{dV}$$

$$\text{Since } V \sim \frac{1}{\rho} \rightarrow K = -\frac{1}{\rho} \frac{dP}{d\left(\frac{1}{\rho}\right)} = -\frac{1}{\rho} \frac{dP}{\frac{-d\rho}{\rho^2}} = \rho \frac{dP}{d\rho}$$

Isothermal bulk modulus

$$K_T = -V \left(\frac{\partial P}{\partial V} \right)_T \equiv \rho \left(\frac{\partial P}{\partial \rho} \right)_T = \frac{1}{\kappa_T}$$

Compressibility

$$\kappa_T = \frac{1}{K_T}$$

$$\kappa_T = \frac{1}{\rho} \left(\frac{\partial \rho}{\partial P} \right)_T$$

Isentropic (adiabatic) bulk modulus

$$K_a = -V \left(\frac{\partial P}{\partial V} \right)_S \equiv \rho \left(\frac{\partial P}{\partial \rho} \right)_S$$

$$\kappa_a = \frac{1}{K_a}$$

$$\kappa_a = \frac{1}{\rho} \left(\frac{\partial \rho}{\partial P} \right)_S$$

Appendix

Young Modulus

For a stretched wire of cross-sectional area A and length L :

$$Y = -\frac{L}{A} \left(\frac{\partial f}{\partial L} \right)_T \quad \left(\mathbf{E} = \frac{\text{Stress}}{\text{Strain}} = \frac{\sigma}{\varepsilon} \right)$$

Shear Modulus

$$\mu = \frac{\tau_{ij}}{\varepsilon_{ij}} \quad i \neq j$$

Appendix

Seismic Velocities

P-Velocity

$$V_P = \left(\frac{K_a + 4\mu/3}{\rho} \right)^{1/2}$$

S-Velocity

$$V_S = \left(\frac{\mu}{\rho} \right)^{1/2}$$

Seismic Parameter

$$\phi = V_P^2 - \frac{4}{3} V_S^2 \equiv \frac{K_a}{\rho}$$

Poisson Ratio

$$\nu = \frac{\epsilon_{trans}}{\epsilon_{axial}}$$

ϵ_{trans} : Transverse strain - positive for tension, negative for compression.

ϵ_{axial} : Axial strain - positive for tension, negative for compression.

$$\nu = \frac{\left(\frac{V_P}{V_S} \right)^2}{2 \left(\frac{V_P}{V_S} \right)^2 - 2}$$

